Examination of the Details of 2D Vorticity Generation Around the Airfoil During Starting and Stopping Phases

Alwin Wang
Supervised By: Hugh Blackburn

25 May 2018

Abstract

This project covers a numerical study of vorticity generation around a 2D airfoil during the starting and stopping phases. It will focus on a single NACA0012 airfoil of unit chord where the two-dimensional Navier-Stokes equations are solved using a spectral element DNS code. Results for a small range of low Reynolds numbers from 1,000 to 50,000 will be examined and the results for a zero-lift angle of attack compared to an angle of attack of four degrees. Vorticity production on the surface and the evolution of leading edge and trailing edge vortex shedding will be analysed. Fast vorticity and slow vorticity generation will be investigated by considering impulsively stated and uniformly accelerated viscous flows. In addition, the contribution of the two vorticity mechanisms, tangential pressure gradients from the fluid side and acceleration of the surface from the wall side, will be compared. Analysis of the results suggest different generation mechanisms dominate different regions on the airfoil surface and observed pair of leading edge vortices and trailing edge vortex. Calculation of the circulation of these vortices allows the vorticity production to be related to the overall life production.

Summary

This report summarises the work conducted in Semester 1 of 2018 on vorticity production around 2D airfoils. Time was conducting a literature review of existing research, configuring Semtex on Ubuntu 16.04 LTS and conducting initial analysis. Files and results from Vincent 2014 were recreated and post-processing using finite difference methods conducted. Additional flow cases with different acceleration profiles and Reynolds numbers were also investigated. It was found that a finite difference scheme would not be suitable to accurately estimate the vorticity gradients and a method using the should be pursued instead.

Contents

1 Introduction

1.1 Background

Although vorticity is not a primary variable in fluid dynamics, it is an important variable for understanding and solving problems (Morton 1984). The Kutta-Joukowski Theorem (Equation 1) helps explain lift production by relating the lift per unit span and circulation – the flux of vorticity (Anderson 2011). Used in conjunction with Kelvin's circulation theorem (shown in Figure 1a), many fundamental textbooks relate the generation of circulation around an airfoil to the starting and stopping vortices at the trailing edge produced by large velocity gradients (Anderson 2011, Torenbeek 2009). Figure 1b shows these stating and stopping vortices as observed in experiments by Prandtl, Tietjens and Müller (1957) over 80 years ago.

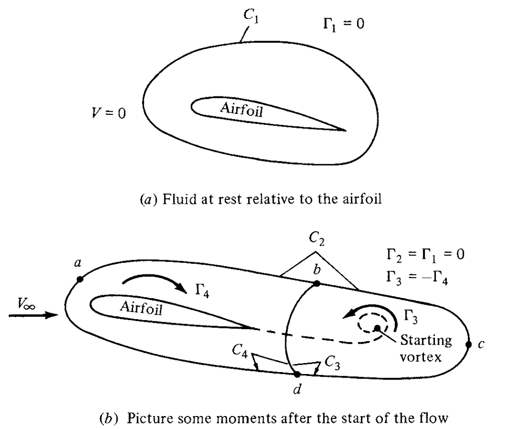

(a) Circulation around an airfoil in inviscid incompressible flow (Anderson, 2011)

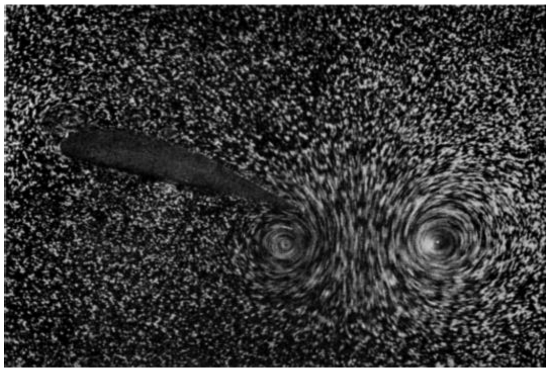

(b) Snapshot from Prandtl's flow visualisation film of a transient lifting airfoil

Figure 1: Vortex shedding from 2D airfoils

$$L' = \rho_\infty V_\infty \Gamma \tag{1}$$

$$\Gamma \equiv -\oint_A \boldsymbol{V} \cdot \mathrm{d}\boldsymbol{s} = -\iint_S (\nabla \times \boldsymbol{V}) \cdot \mathrm{d}\boldsymbol{S} = -\iint_S \omega \cdot \mathrm{d}\boldsymbol{S} \tag{2}$$

With the increase in availability of computational power in recent decades, multiple numerical studies have been conducted on vorticity production around an airfoil. In addition to Prandtl's main findings, other phenomena have been discovered in relation to vortex production and shedding. Numerical studies of viscous starting flows past wedges conducted by Xu (2016) detailed vorticity evolution which is applicable to finite-angle trailing edges of airfoils. For low Reynolds number airfoils Lei, Feng and Can (2013) discovered laminar separation bubbles on the upper surface that could cause periodic primary and secondary vortex shedding that varied with angle of attack. Leading edge vortices were also observed by Vincent and Blackburn (2014) on airfoils during the stopping phase which questions the importance of vortex production on airfoil regions other than the trailing edge. Though there is an emphasis in current literature on vorticity generation at the trailing edge, this project will take a more holistic approach to investigating vorticity generation around the entire surface to better understand these phenomena.

During the starting and stopping phases of motion the airfoil, the vorticity production is due to the relative acceleration of the fluid and wall. It is recognised that the sources of vorticity must occur at the boundary of the fluid regions. For this particular case, Morton (1984) outlines two production mechanisms as tangential pressure gradients from the fluid side and acceleration of the surface from the wall side. In either mechanism the vorticity is generated instantaneously and partially masked by viscous diffusion when there is constant generation (Morton 1984). These contributions were investigated by Blackburn and Henderson (1999) for vortex shedding of oscillating cylinders and it was noted the pressure-gradient generation mechanism could override the surface-acceleration generation mechanism and vice versa.

As such, the Navier-Stokes equation (shown in Equation 3) can be reduced to the case of a wall moving in its own plane for an infinitesimally small region on the airfoil (coordinate system defined in Figure 2) as described by Morton (1984). The boundary conditions for the Navier-Stokes equation were found by using $\boldsymbol{V} = \{U(t), 0\}$ where $U(t)$ is the motion of the body and $z = 0$ to indicate the rigid boundary at the wall. Thus, no slip condition gives $\boldsymbol{v} = (U(t), 0)\ \forall\, x, t$ for the fluid at the wall and there is no spatial variation of the boundary motion (shown in Equation 4). Substitution into the Navier-Stokes equation at the boundary yields Equation 5a which can be simplified to Equations 5b and 5c (Morton, 1984).

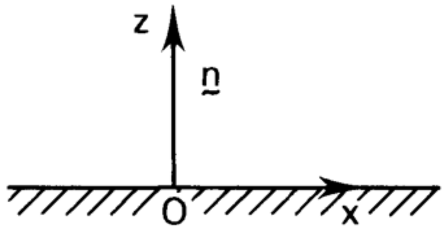

Figure 2: Definition of coordinate system (Morton, 1984)

$$\frac{\partial \boldsymbol{u}}{\partial t} + \boldsymbol{u}\cdot\nabla\boldsymbol{u} = -\frac{1}{\rho}\nabla\rho + \frac{1}{\mathrm{Re}}\nabla^2\boldsymbol{u} - \boldsymbol{a}, \qquad \nabla\cdot\boldsymbol{u} = 0 \tag{3}$$

$$\left[\left(\frac{\partial}{\partial x}, \frac{\partial^2}{\partial x^2}\right)\cdot(u, w)\right]_0 = 0 \tag{4}$$

$$\left[\frac{\partial^2}{\partial z^2}(u, w)\right]_0 = \left\{0, \frac{1}{\mu}\frac{\partial \boldsymbol{p}}{\partial x} + \frac{1}{\nu}\frac{d\boldsymbol{U}}{\mathrm{d}t}, \frac{1}{\mu}\right\}_0 \tag{5a}$$

$$\nu\left(\frac{\partial\omega}{\partial z}\right)_0 = \left\{0, -\left[-\frac{1}{\rho}\frac{\partial \boldsymbol{p}}{\partial x} + \frac{d\boldsymbol{U}}{dt}\right], 0\right\}_0 \tag{5b}$$

$$-\nu\boldsymbol{n}\cdot\nabla\omega = -\boldsymbol{n}\times(\nabla\boldsymbol{P} + \boldsymbol{a}) \tag{5c}$$

1.2 Project Aims

This project will explore the vortex generation around an airfoil during acceleration and deceleration of the airfoil which has observed in earlier research. The first aspect of this project will require a literature review to appreciate the various phenomena already recorded and recreate them in a numerical simulation. The next aspect of this project will analyse the contributions of the two vorticity generation mechanisms for various regions of the airfoil surface (Equation 5c) and how variables such as Reynolds number and acceleration affect the generation mechanism. The last aspect of the investigation will involve varying parameters such as the Reynolds number and calculating the strengths of various vortices produced around the airfoil by evaluating Equation 2.

2 Work Complete

2.1 Methodology

The scope of this project will be limited to two dimensional flows to reflect the initial Prandtl experiments and compare results to established literature. For similar reasons, low Reynolds numbers will be used, specifically between 1,000 and 50,000. Finally, the initial analysis will be limited to numerical simulations of a single airfoil, NACA0012, at a single angle of attack, 4 degrees. While this does reduce the capacity of this project it does reduce the computational resources required which allows for much finer investigation of time, Reynolds number, pressure gradient, acceleration and vorticity. The equations to be numerically solved are the two-dimensional incompressible Navier-Stokes equations in the acceleration reference frame shown in Equation 3 and the vorticity strength in the inertial reference frame at the surface of the airfoil shown in Equation 5b (Morton 1984).

Figure 3 shows the mesh used in the initial analysis of the NACA0012 at an angle of attack 4 degrees. This mesh is the same as the mesh used by Vincent 2014 and was used as a baseline to ensure the same results were obtained before moving to further detailed analysis.

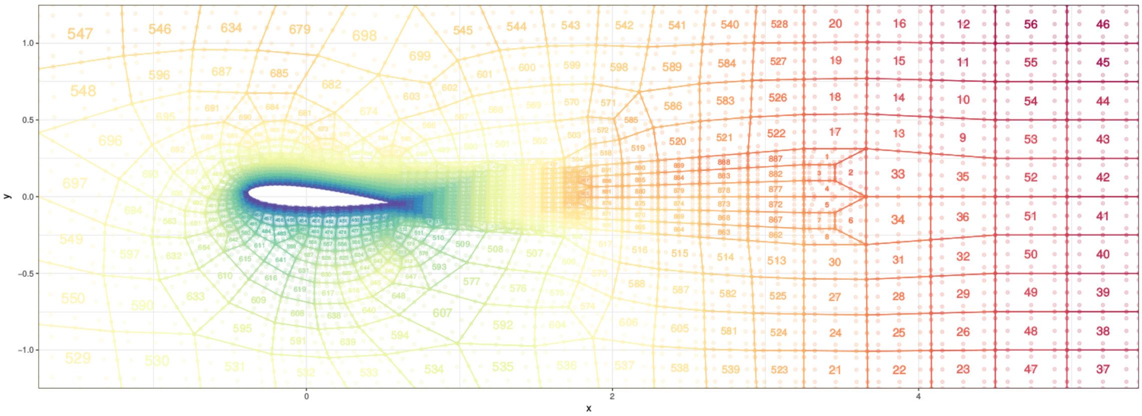

Figure 3: Mesh for NACA0012 at angle of attack 4 degrees (mesh source: Vincent, 2014)

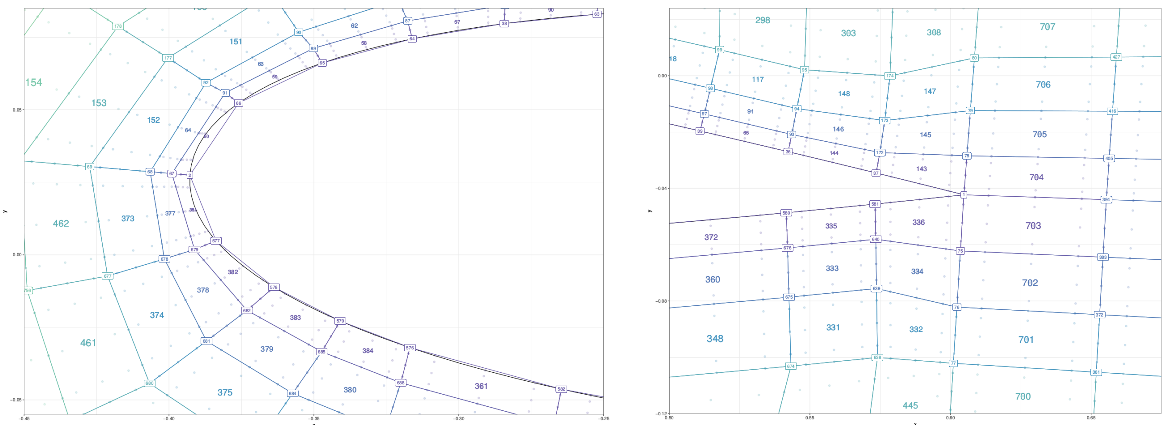

(a) Leading Edge

(b) Trailing Edge

Figure 4: Output of 4th order polynomial mesh overlaid on session file of defined elements and nodes in the semtex session file

From Equation 5b it was evident that the gradients of the vorticity and pressure were required.

However, from figure 4 it was evident that the mesh was not constructed such that mesh lines were tangential and orthogonal to the airfoil surface. For the initial analysis it was decided that points normal to the surface would be taken and the value of vorticity interpolated using a bicubic spline method. These points would then be used to estimate $\left(\frac{\partial \omega}{\partial z}\right)_0$ using a one-sided finite difference method for five equally spaced points, $z_0, z_{+1}, \ldots, z_{+4}$, such that the error would be similar in magnitude to the polynomial order chosen (shown in Equation 6) (Fornberg, 1988).

$$\frac{\partial \omega}{\partial z}(z_0) \approx \frac{-\frac{25}{12}\omega(z_0) + 4\omega(z_{+1}) - 3\omega(z_{+2}) + \frac{4}{3}\omega(z_{+3}) - \frac{1}{4}\omega(z_{+4})}{h} + O\left(h_z^4\right) \tag{5}$$

For the bicubic interpolate of points, $z_0, z_{+1}, \ldots, z_{+4}$, it was quickly discovered that the interpolation would not provide accurate results at the trailing edge. This was because a triangulation algorithm was used to determine the interpolation for irregularly spaced data. As such, a point that lay in an element on the lower surface, e.g. element 336, may use point(s) from the upper surface, e.g. element 143, as part of the triangulation.

One solution to this problem was to transform the field properties (x, y, u, v, p, ω) into a coordinate system normal and tangential to the surface of the airfoil before interpolation. However, it was found that this coordinate transformed introduced too much error as shown in Figure 5. The solution for this problem was to use a point-in-polygon algorithm (O'Rourke, 1998) to first determine which element a point lay in. When the interpolation was run, only the points within that element would be used in the interpolation. While this prevented 'wrong' points being used, it did not guarantee smooth results at the boundary of elements.

An estimate of the interpolation error was determined by using the interpolated values to estimate the value of ω on the original mesh points (x, y). These results were consistent with Figure 5, if the field was first transformed into a normal and tangential grid (similar to conformal mapping), the average error was 204.4% with standard deviation 5923.1% whereas interpolating on each element individually gave an average error of -1.13 % with standard deviation 76.6% (for this particular time step).

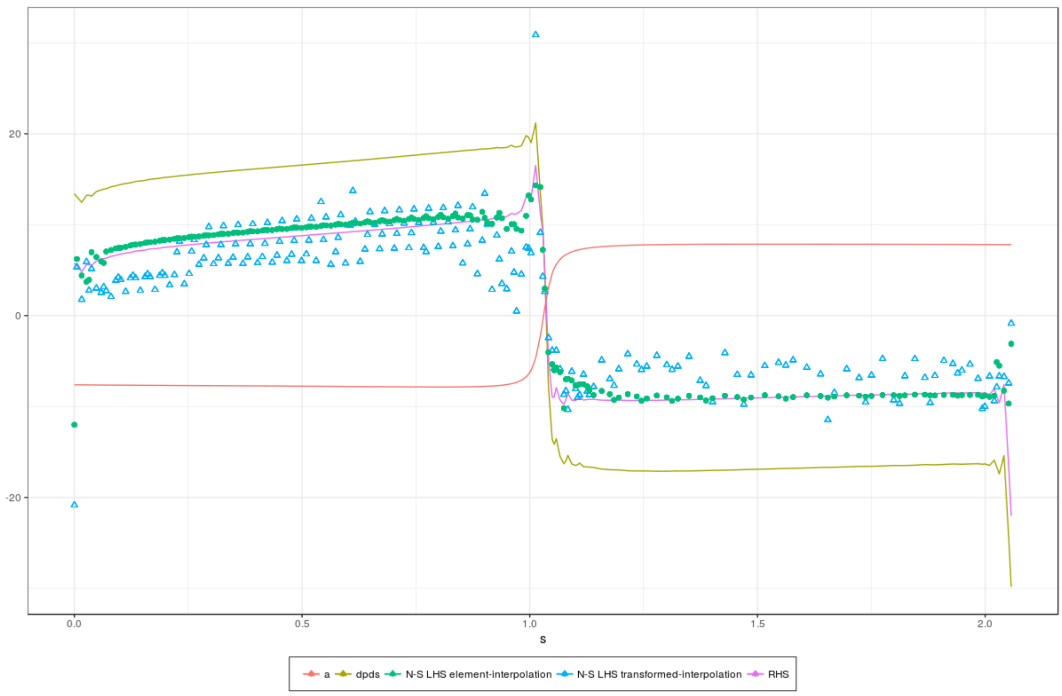

Figure 5: Comparison of two interpolation methods at $t = 0.1$ for $Re = 10,000$.

2.2 Results

For each case of fast and slow vorticity generation three Reynolds numbers were considered, 1,000, 5,000 and 10,000. Figures 6 and 7 on the following pages show the results of the numerical simulation and the post processing using the finite difference of points interpolated normal to the airfoil surface. For these plots, the method of interpolation was to interpolate per element as this was found to be more accurate earlier.

However, for both the impulsively and non-impulsively started flow cases, it can be seen that there is a clear discrepancy between the left hand side of Equation 5b and the right hand side of Equation 5b at lower Reynolds numbers. Even when the points for interpolation were moved closer to the surface, this discrepancy remained.

2.3 Limitations

Due to the apparent error between the left hand side and right hand side of the theoretical result in Equation 5b, it was determined that even this interpolation post-process method was inadequate.

The proposed solution is to use the underlying piecewise polynomials in semtex to generate a vector field of pressure and vorticity gradients. Rather than using Equation 5b where the derivatives are taken in directions normal and perpendicular to the surface, Equation 5c will be used instead to take the cross product between the normal vector and the vector field of derivatives.

As this semtex is a spectral element solver, this would mean that each element has its own set of basis polynomial functions. While primary variables (u, v, p) are continuous across element boundaries, derived variables like vorticity are not guaranteed to be continuous. Thus, care should be taken to ensure that the vorticity is continuous across element boundaries such that the vorticity gradient is not affected. This can be achieved by increasing the polynomial order.

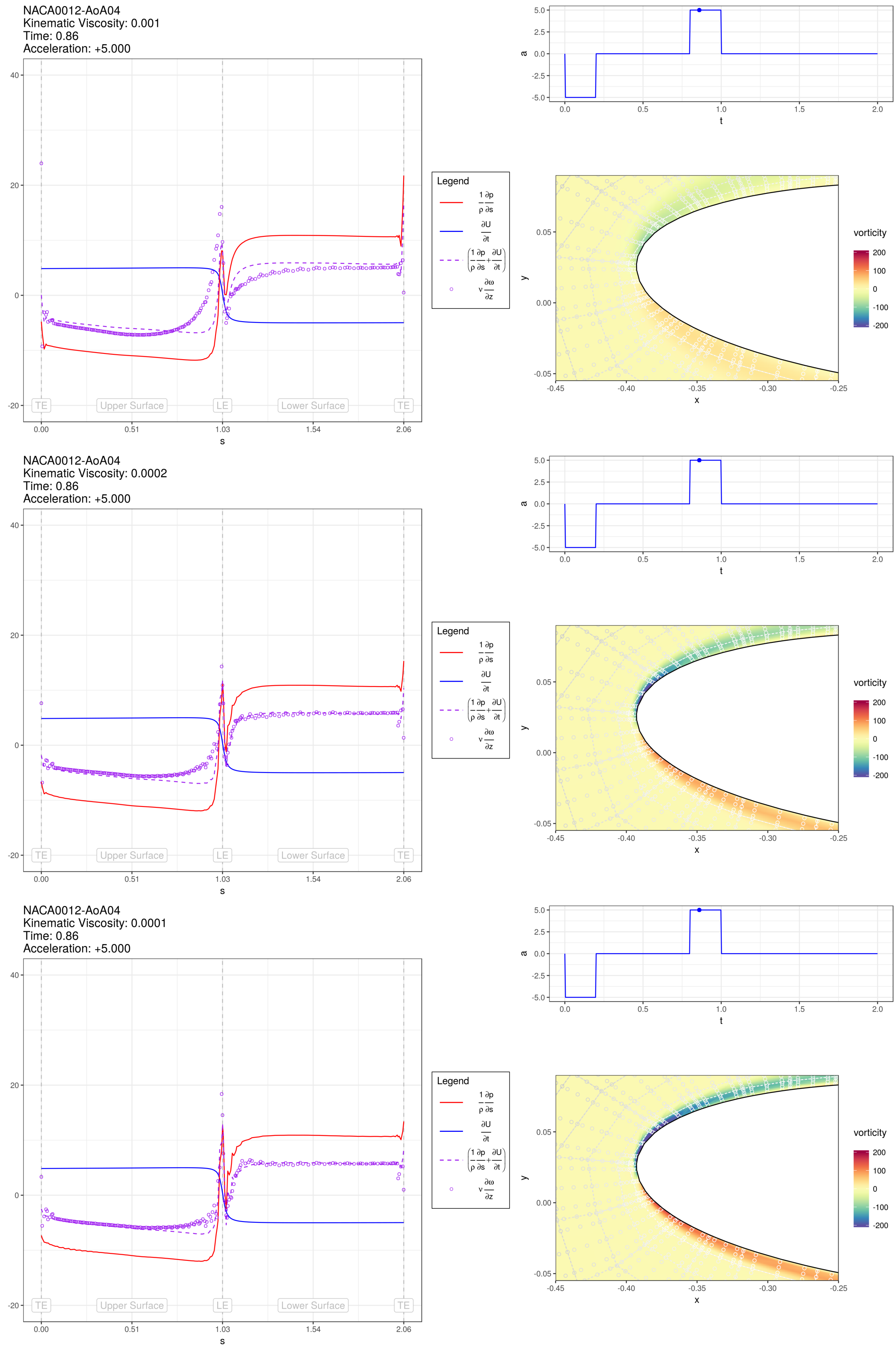

Figure 6: Impulsively started flow at t = 0.86 for Re = 1000, 5000, 10000

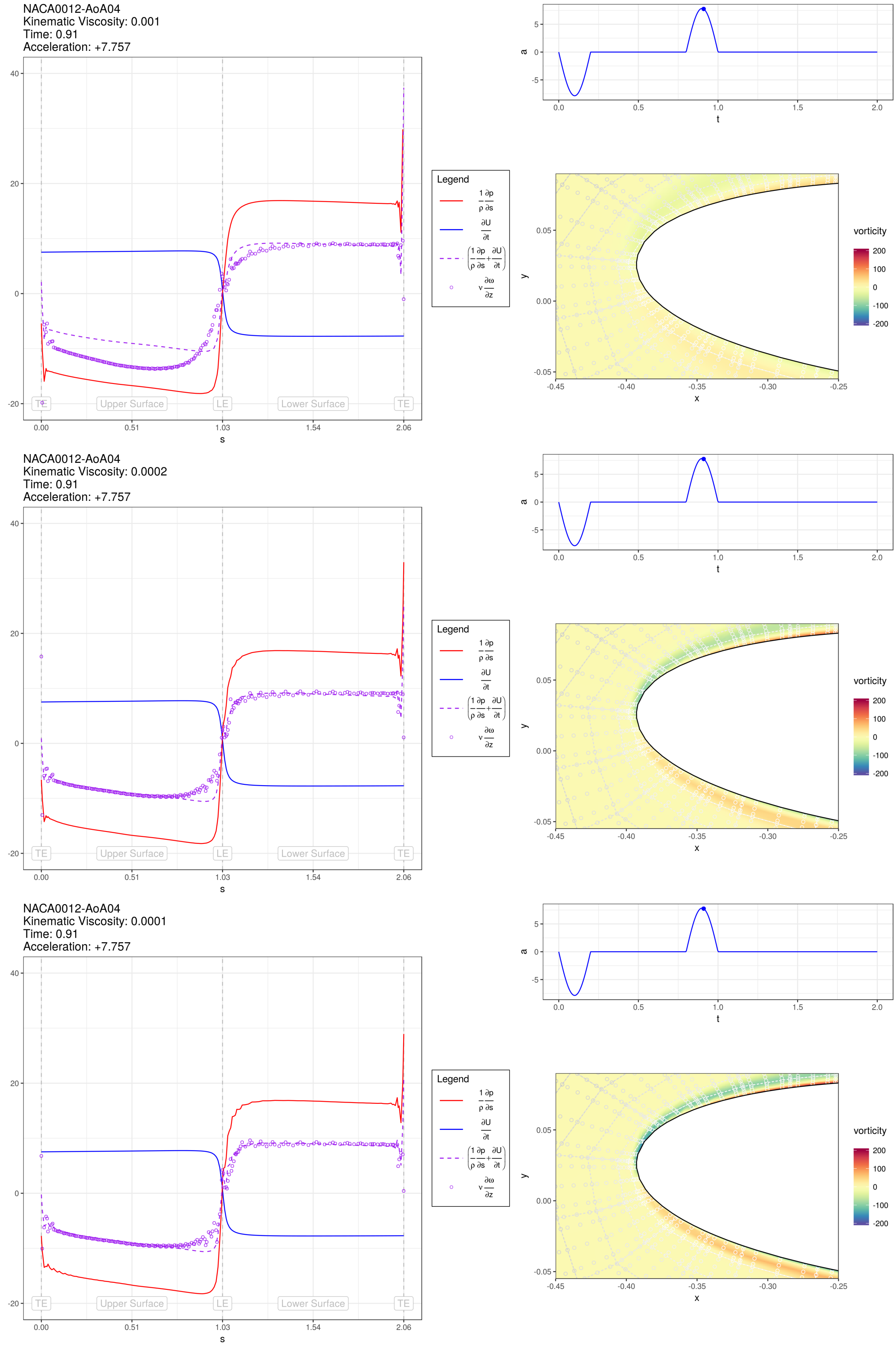

Figure 7: Non-Impulsively started flow at t = 0.91 for Re = 1000, 5000, 10000

3 Work Planned

3.1 Project Plan

Unfortunately, there is still a large amount of work remaining. While progress has been on track with the initial plan in the project proposal, the difficulties in accurately estimating the vorticity and pressure gradients is a significant setback.

The next major focus will be to try to incorporate the post-processing into semtex as an additional utility function. This will require an understanding of semtex's inner workings and spectral elements methods. However, by using the piecewise polynomial basis functions in the Galerkin method, it should result in a more accurate estimation. Care should be taken at the boundaries of elements as it is not guaranteed that the vorticity (or other derived quantities) will be constant).

The next steps will be to analyse the results as per Equation 5b to investigate the vorticity generation mechanisms and their dependence on variables such as location and acceleration.

Two extension ideas have been identified which are a non-lifting airfoil, i.e. NACA0012 at zero angle of attack, and a cylinder to determine the effects of lift production and a sharp trailing edge on the vorticity generation around a surface.

3.2 Timeline

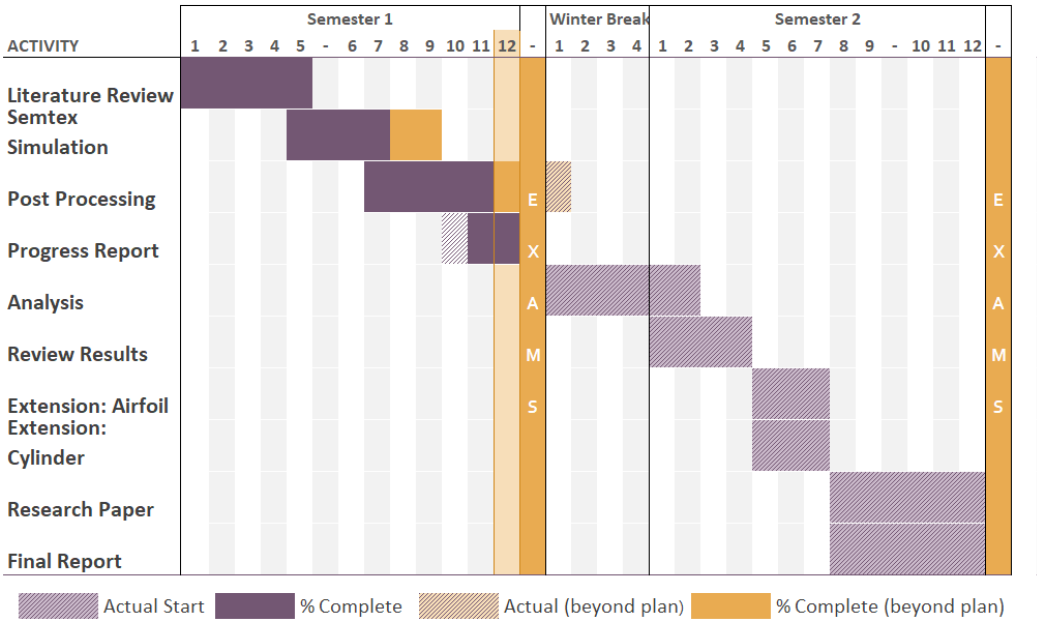

Figure 8: Updated timeline

4 Conclusion

An initial analysis has been conducted on a single NACA0012 airfoil at angle of attack 4 degrees. It was found that the chosen method of estimating derivatives using a finite difference method was inadequate and an alternative approach should be chosen to ensure better quality results.

5 References

Anderson, J.D., 2011. *Fundamentals of aerodynamics* 5th ed., NY McGraw-Hill, pp 174-177, 280-282, 330-338.

Blackburn, H. M. & Henderson, R. D. 1999. *A study of two-dimensional flow past an oscillating cylinder*, Journal of Fluid Mechanics, Vol 385, pp. 255-286.

Blackburn, H. M. & Sherwin S. J. 2004. *Formulation of a Galerkin spectral element–Fourier method for three-dimensional incompressible flows in cylindrical geometries*, Journal of Computational Physics, Vol 197, pp. 759–778.

Jones, A. & Babinsky, H. 2011. *Reynolds number effects on leading edge vortex development on a waving wing*, Exp Fluids 2011, pp. 197-210.

Fornberg, B. 1988. *Generation of Finite Difference Formulas on Arbitrarily Spaced Grids*, Mathematics of Computation, 51 (184) pp 699–706.

Lei, J., Feng, G. & Can, H. 2013. *Numerical study of separation on the trailing edge of a symmetrical airfoil at a low Reynolds number*, Chinese Journal of Aeronautics, pp.918-925.

Morton, B. R. 1984. *The generation and decay of vorticity*, Geophys. Astrophys. Fluid Dyn., Vol 28, pp. 277-308.

Noca, F., Shiels, D. & Jeon, D. 1999. *A Comparison of Methods for Evaluating Time-Dependent Fluid Dynamic Forces on Bodies, Using Only Velocity Fields and Their Derivatives*, Journal of Fluids and Structures, Vol 13, pp 551-578.

O'Rourke, J. 1998. *Computational Geometry in C* 2nd ed., Cambridge University Press.

Prandtl, L & Tietjens, O.G., *Applied Hydro- and Aeromechanics, Engineering Societies Monographs*, 1934.

Torenbeek, E., Wittenberg, H & SpringerLink, 2009. *Flight physics: Essentials of aeronautical disciplines and technology, with historical notes*, London: Springer, pp 137-148.

Vincent, M. 2014. *Simulation of starting/stopping vortices for a lifting airfoil*, 19th Australasian Fluid Mechanics Conference, 8-11 December, Melbourne, Australia.

Xu, L., 2016. *Numerical study of viscous starting flow past wedges, Journal of Fluid Mechanics*, Vol 801, pp 150-165.